

GAZI

JOURNAL OF ENGINEERING SCIENCES

Experimentally Assessing the Wear Characteristics of 3D-Printed PLA and Tough PLA Materials Based on Fused Deposition Modeling

Engin Tan^{a*}

Submitted: 14.06.2023 Revised: 18.07.2023 Accepted: 09.08.2023 doi:10.30855/gmbd.0705065

ABSTRACT

Keywords: Wear, PLA, tough PLA, fused deposition modeling, 3D-printing

^{a,*} Pamukkale University,
Faculty of Technology,
Dept. of Metallurgical
and Materials Engineering
20160 - Denizli, Türkiye
Orcid: 0000-0003-4441-3678
e mail: etan@pau.edu.tr

*Corresponding author:
etan@pau.edu.tr

This study investigated the wear properties of two commonly utilized polymer materials, PLA (Poly Lactic Acid) and Tough PLA, in additive manufacturing applications. The samples were produced with a 100% infill rate on a 3D printer using Fused Deposition Modeling. Hardness measurements and abrasive wear tests were conducted to analyze the wear characteristics of the samples. The comparison involved parameters such as volume loss, coefficient of friction, and specific wear rate. Additionally, surface roughness measurements were performed to assess the quality of the worn surfaces. Wear maps were constructed to obtain information about the wear mechanisms, and scanning electron microscopy and energy-dispersive X-ray spectroscopy were used to describe the worn surfaces. The results demonstrated that Tough PLA exhibited superior wear resistance compared to PLA. The highest volume loss of 3.75 mm³ was observed in the PLA-5 m/s sample under a 15 N load, whereas the lowest of 0.55 mm³ was in the Tough PLA-1.5 m/s sample under a 5 N load. Depending on the applied load and sliding distances, fatigue, micro-fracture, and micro-cutting mechanisms were identified as contributing factors to the wear process. Furthermore, it was observed that higher applied loads resulted in a significant increase in surface roughness values.

Eriyik Yiğma Modellemeye Dayalı 3B Baskılı PLA ve Tok PLA Malzemelerinin Aşınma Özelliklerinin Deneysel Olarak Değerlendirilmesi

ÖZ

Bu çalışma, eklemeli imalat uygulamalarında yaygın olarak kullanılan iki polimer malzemenin, PLA (Poli Laktik Asit) ve Tough PLA'nın aşınma özelliklerini araştırmıştır. Numuneler, Eriyik Yiğma Modelleme kullanılarak bir 3D yazıcıda %100 doluluk oranıyla üretildi. Numunelerin aşınma özelliklerini analiz etmek için sertlik ölçümleri ve aşındırma aşınma testleri yapılmıştır. Karşılaştırma, hacim kaybı, sürtünme katsayısı ve özgül aşınma oranı gibi parametreleri içeriyordu. Ayrıca aşınmış yüzeylerin kalitesini değerlendirmek için yüzey pürüzlülük ölçümleri yapılmıştır. Aşınma mekanizmaları hakkında bilgi elde etmek için aşınma haritaları oluşturuldu ve aşınmış yüzeyleri tanımlamak için taramalı elektron mikroskopu ve enerji dağıtıcı X-ışını spektroskopisi kullanıldı. Sonuçlar, Tough PLA'nın PLA'ya kıyasla üstün aşınma direnci sergilediğini gösterdi. En yüksek hacim kaybı 3,75 mm³ ile PLA-5 m/s örneğinde 15 N yük altında gözlenirken, en düşük hacim kaybı 0,55 mm³ ile Tough PLA-1,5 m/s örneğinde 5 N yük altında gözlemlendi. Uygulanan yüke ve kayma mesafelerine bağlı olarak yorulma, mikro kırılma ve mikro kesme mekanizmaları aşınma sürecine katkıda bulunan faktörler olarak belirlenmiştir. Ayrıca, uygulanan daha yüksek yüklerin yüzey pürüzlülük değerlerinde önemli bir artışa neden olduğu gözlemlenmiştir.

Anahtar Kelimeler: Aşınma, PLA, Tok PLA, Eriyik yiğma Modelleme, 3B baskı

1. Introduction

Additive Manufacturing (AM) has emerged as an adaptable technology, facilitating the creation of intricate components with remarkable accuracy and efficiency. The research dedicated to AM technologies has witnessed a substantial growth in recent years. This technology allows for the successful creation of target prototypes from CAD model information and facilitates the production of small-scale components for system modification, repair, and maintenance [1, 2]. AM technology finds extensive applications across various fields, including manufacturing, engineering, aviation, space, and medicine, due to its exceptional 3D-printing capabilities. AM presents a broad spectrum of processes that harness the capabilities of polymers, ceramics, metals, alloys, and composites. This versatility allows for the development of various types of products and components, catering to diverse industry needs and requirements [3-5]. Among these processes, Fused Deposition Modeling (FDM) stands out for its ability to efficiently and cost-effectively produce high-precision layered structures using polymeric engineering materials [6]. FDM excels in delivering fast production rates while maintaining high dimensional accuracy within narrow tolerances [7]. Despite these advantageous features, the layered production in FDM can introduce different surface roughnesses that may pose challenges to the strength characteristics and ergonomics of the produced parts. In addition to traditional materials like ABS and PLA, FDM technology also accommodates polymer-based materials such as PETG, PEKK, PEI, PPSU, and PC, which offer high strength and thermal resistance [8].

PLA is widely utilized in various industries due to its exceptional strength properties, good surface quality, high printing speeds, and cost-effectiveness. Furthermore, its biocompatibility and biodegradability have propelled it to the forefront as the preferred thermoplastic in sectors ranging from food and cosmetics to biomedical applications [9-11]. However, PLA filaments used in FDM technology have certain drawbacks, primarily brittleness, which negatively impacts wear resistance, fracture toughness, and impact resistance. To address these limitations, the development of Tough PLA with enhanced toughness properties has gained attention in recent years. Tough PLA offers unique material characteristics, including improved toughness and enhanced impact resistance, which are crucial for enhancing engineering applications [12]. Compared to standard PLA filaments, Tough PLA filaments exhibit up to three times higher energy dissipation capacity. In addition, the exceptional flexibility of Tough PLA allows it to withstand high levels of friction and impact, making it highly appropriate for an array of engineering purposes. [13-15].

The wear behavior of PLA and Tough PLA produced using FDM technology has received limited research attention. Karabeyoğlu et al. [16] conducted a study investigating the wear behavior of PLA-copper composites. The study revealed that at low temperatures, the wear mechanism was primarily attributed to the abrasive effect caused by copper particles detaching from the surface. Conversely, adhesive wear properties were observed at high temperatures. İstif [17] examined the dry sliding wear behavior of FDM-produced PLA parts. Two different manufacturing directions were selected for PLA samples. The study found that vertically oriented pins experienced significantly higher weight loss compared to horizontally oriented ones, highlighting the significant influence of layer direction on the wear mechanism. Yilmaz [18] examined the adhesive wear behaviours of 3D-printed PETG, ABS, and PLA materials. It was determined that PLA exhibited the lowest wear performance among all the tested materials, while PETG demonstrated the highest resistance to adhesive wear. Sevil et al. [19] investigated three alternative powder and epoxy based coating techniques to develop the wear resistance of 3D-printed PLA items against surface scratches. Erosive wear tests were performed on the coated samples, revealing that the PLA part coated with aluminum oxide powder exhibited the highest erosion rate, while the garnet-coated PLA specimen demonstrated the lowest erosion rate. In a study by Rajesh et al. [20], the dry sliding abrasive wear behavior of PLA and ABS samples produced using FDM was compared. ABS exhibited a higher wear rate and friction force compared to PLA.

In this study, wear samples were fabricated using commercially available PLA and Tough PLA filaments through the FDM 3D-printing method. Abrasive wear tests were conducted on the produced samples, varying the loads, sliding velocities, and sliding distances. The wear behavior of the samples was assessed by analysing parameters such as coefficient of friction, volume loss, and specific wear rate. Surface roughness assessments were utilized to assess the current condition of the worn surfaces. Additionally, SEM and EDS investigations were used to characterize the worn surfaces. Unlike the existing literature studies, in this study, a wear mechanisms map was created to contribute to the optimization of the wear behavior of PLA and to help determine the appropriate wear conditions.

2. Experimental Procedure

For this study, two filament materials, namely PLA and Tough PLA, were obtained from Porima Polymer Technologies Inc. located in Turkey. Table 1 shows the manufacturing specifications of the filaments as reported by the company. Furthermore, Table 2 describes the physical, thermal, and mechanical features of the filaments.

Table 1. Production parameters of the filaments

| Materials | Colors | Diameter (mm) | Processing Temperature (°C) | Platform Temperature (°C) |
|-----------|--------|---------------|-----------------------------|---------------------------|
| PLA | Brown | 1.75 | 200-230 | 60-75 |
| Tough PLA | Black | | | |

Table 2. The physical, thermal, and mechanical features of the filaments

| Features | PLA | Tough PLA |
|--|-------|-----------|
| Heat Bending Temperature (°C) | 55 | 58 |
| Glass Transition Temperature (°C) | 55-60 | 55-65 |
| Density (g/cm ³) | 1.23 | 1.22 |
| Melt Flow Index (g/10min) | 17.3 | 17.3 |
| Tensile Strength (MPa) | 56 | 50 |
| Young Modulus (MPa) | 2850 | 2400 |
| Elongation at Break (%) | 7 | 50 |
| Notch Impact Energy (kJ/m ²) | 14.2 | 36 |

Wear samples of PLA and Tough PLA were fabricated using the FDM method on the Ender 3 Pro 3D printer, with dimensions of Ø10x20 mm. Figure 1 provides a schematic image of the production process, along with a photograph of the printer used. Detailed information regarding the FDM parameters for 3D printing can be found in Table 3.

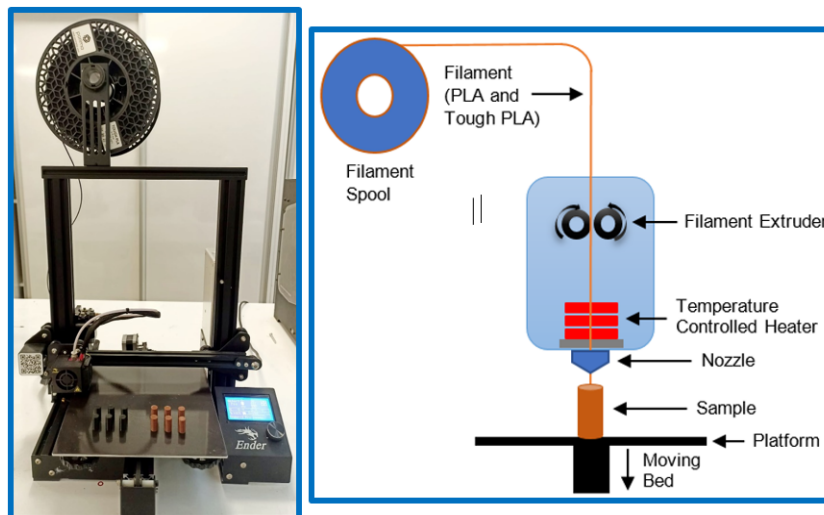


Figure 1. Production process of samples via 3D-printer

Table 3. The physical, thermal, and mechanical features of the filaments

| Parameters | PLA | Tough PLA |
|---------------------------|---------|-----------|
| Platform Temperature (°C) | 60 | 65 |
| Nozzle Temperature (°C) | 215 | 225 |
| Nozzle Diameter (mm) | 0.4 | 0.4 |
| Layer Thickness (mm) | 0.20 | 0.20 |
| Infill Rate (%) | 100 | 100 |
| Print Speed (mm/s) | 75 | 60 |
| Raster angle (°) | +45/-45 | +45/-45 |

Several factors impact the quality of objects created using 3D printing technology, including the cohesiveness among printed layers. Control over the platform temperature is crucial for ensuring optimal part quality. In this study, to avoid distortion and potential thermal stresses, The PLA platform temperature has been fixed at 60 °C and the Tough PLA platform at 65 °C. Notably, the nozzle temperature for Tough PLA was higher than PLA due to its lower viscosity, which increases the risk of clogging during extrusion through the nozzle [21, 22]. Furthermore, Gurrala et al. [23] and Singh et al. [24] have highlighted the significance of the raster angle in reducing damage caused by adhesions between interlayers during the 3D-printing process. Thus, a raster angle of 45°/-45° was selected for this study. The ambient room temperature during printing was maintained between 20 and 25 °C, with a relative humidity of approximately 50%. After completion of the printing process, the 3D-printed samples were stored under laboratory conditions for 96 hours to comply with the ASTM D618 standard. To account for variations in dimensional tolerances resulting from different parameter settings in the 3D printing process, measurements were taken from five different points in the diameter and height regions of each sample using a digital caliper. The dimensional accuracy was determined to be at least 99%.

Hardness measurements were evaluated using the Shore D method, following the ASTM 2240-15 standard guidelines. A Durotronic 1000 Model Shore D-type durometer was used for hardness measurements. Five different measurements were averaged across the diameter sections of the wear samples to ensure consistent hardness values on the sample surfaces.

The abrasive wear tests were conducted following the ASTM G99 standard, employing the pin-on-disc method. The samples were securely fixed onto the Turkeyus PODWT tribometer, as depicted in Figure 2, and subjected to an abrasion test utilizing 800-grit sandpaper.

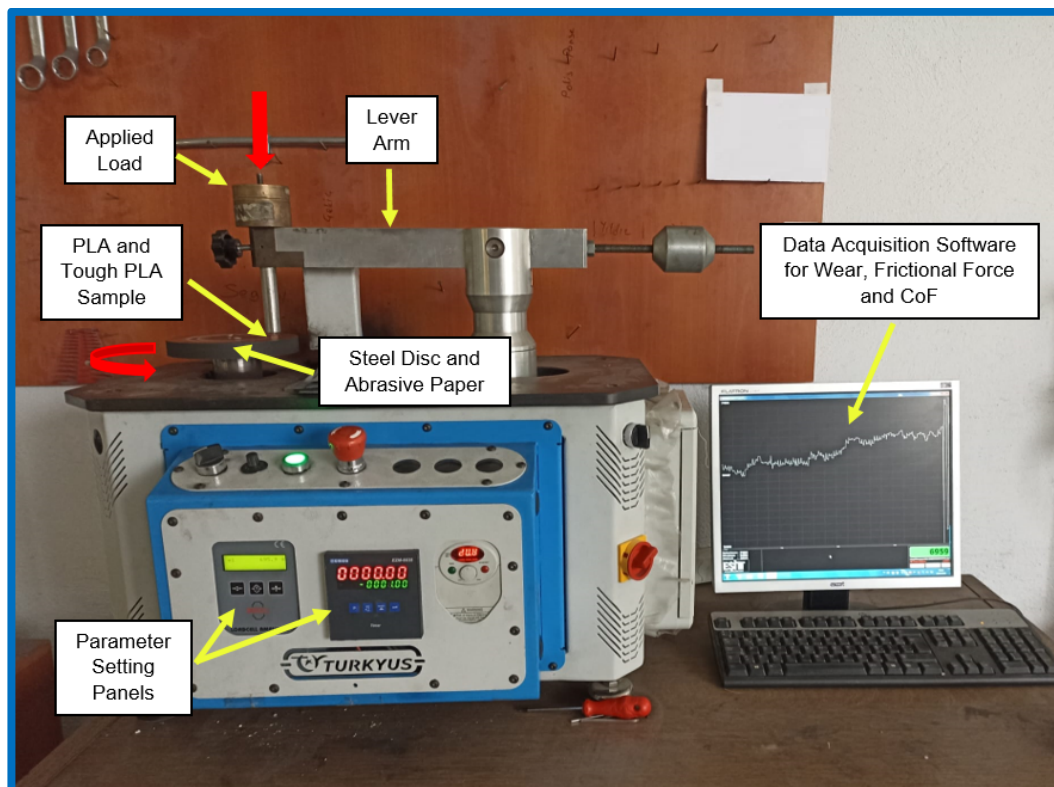


Figure 2. Pin on disc tribometer used in wear tests

The dry sliding wear tests were performed under varying conditions, including 5, 10, and 15 N loads, sliding velocities of 1.5, 3, and 5 m/s, and sliding distances of 100, 200, and 300 m. The friction forces were measured during the wear testing using the Esit Data Logger software, which has been incorporated into the pin-on-disc apparatus. These measurements enabled the determination of the coefficient of friction, volume loss, and specific wear rate. The coefficient of friction (CoF) was calculated using Equation 1, the volume loss (V , mm^3) was evaluated using Equation 2, and the specific wear rate (SWR, $\text{mm}^3 \cdot \text{N}^{-1} \cdot \text{m}^{-1}$) was calculated using Equation 3. The obtained wear test results were

then subjected to further analysis.

$$CoF = F/P \quad (1)$$

; F is the friction force (N) and P is the applied normal load (N).

$$V = m/\rho \quad (2)$$

; m is the mass loss (g) and ρ is the density (g/cm^3).

$$SWR = V/P.L \quad (3)$$

; L is the total sliding distance (m) [25].

Surface roughness data were investigated using the Hardway 462 roughness tester to evaluate the condition of the worn surfaces after the wear tests. The wear mechanisms were determined by creating a wear map depending on the volume loss. This map provided valuable information about the specific wear mechanisms that emerged during testing. Characterization analyses were performed using a Zeiss Supra 40VP high-resolution SEM to correlate worn surface morphologies with wear mechanisms.

Furthermore, EDS analyses were conducted to examine the elemental content distributions within the worn surfaces. These analyses yielded valuable information regarding the presence and distribution of various elements on the surfaces that underwent wear.

3. Results and Discussion

3.1. Hardness

A comparison of hardness values between the PLA and Tough PLA samples is illustrated in Figure 3. The PLA sample displayed the highest hardness, measuring 83.6 Shore D with a mean standard deviation of 1.45. Conversely, the Tough PLA sample exhibited the lowest hardness, measuring 79.3 Shore D with an average standard deviation of 0.95. These findings are consistent with previous literature data [13, 15]. Notably, the difference in hardness was not significantly influenced by the layer thickness [1]. However, Tough PLA demonstrated improved layer adhesion, toughness, and surface quality compared to PLA. These favorable properties also contribute to the stability of the measured hardness results [26]. It is worth mentioning that any defects present in the 3D-printed parts, such as openings, cracks, voids, or air gaps, can affect the mean and standard deviation data [27]. The interactions between molecules formed between the additive and the PLA matrix have a direct impact on the hardness of PLA. Hardness rises when the additive is homogenous diffused and distributed throughout the matrix, showing stronger intermolecular interactions. Furthermore, proper filler distribution improves load transmission between layers. Inadequate dispersion of the additive, on the other hand, might result in infill agglomeration, which reduces the interactions between molecules among PLA and the additive [28]. As a result, there is a reduction in hardness.

In conclusion, Tough PLA is formulated with a lower hardness than PLA to optimize its toughness, wear resistance, and impact strength properties.

3.2. Wear behaviours and mechanisms

The wear behaviors of PLA and Tough PLA were investigated in relation to the applied load and volume loss. Figure 4 illustrates the direct influence of the applied load on wear resistance, resulting in increased volume loss. However, it was observed that sliding under high loads can reduce wear, while low loads tend to exhibit a combination of retention and sliding mechanisms [29].

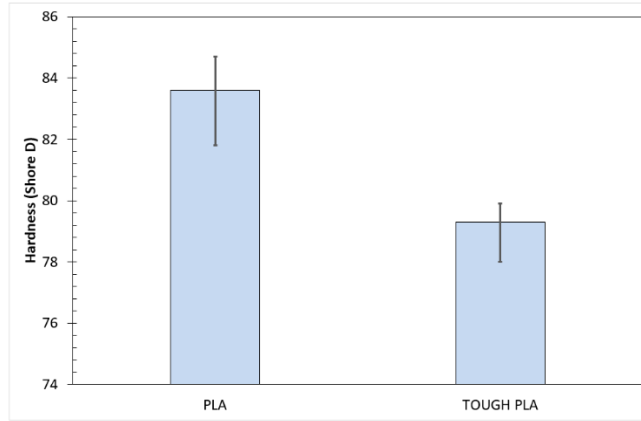


Figure 3. Hardness comparison of FDM 3D-printed wear samples

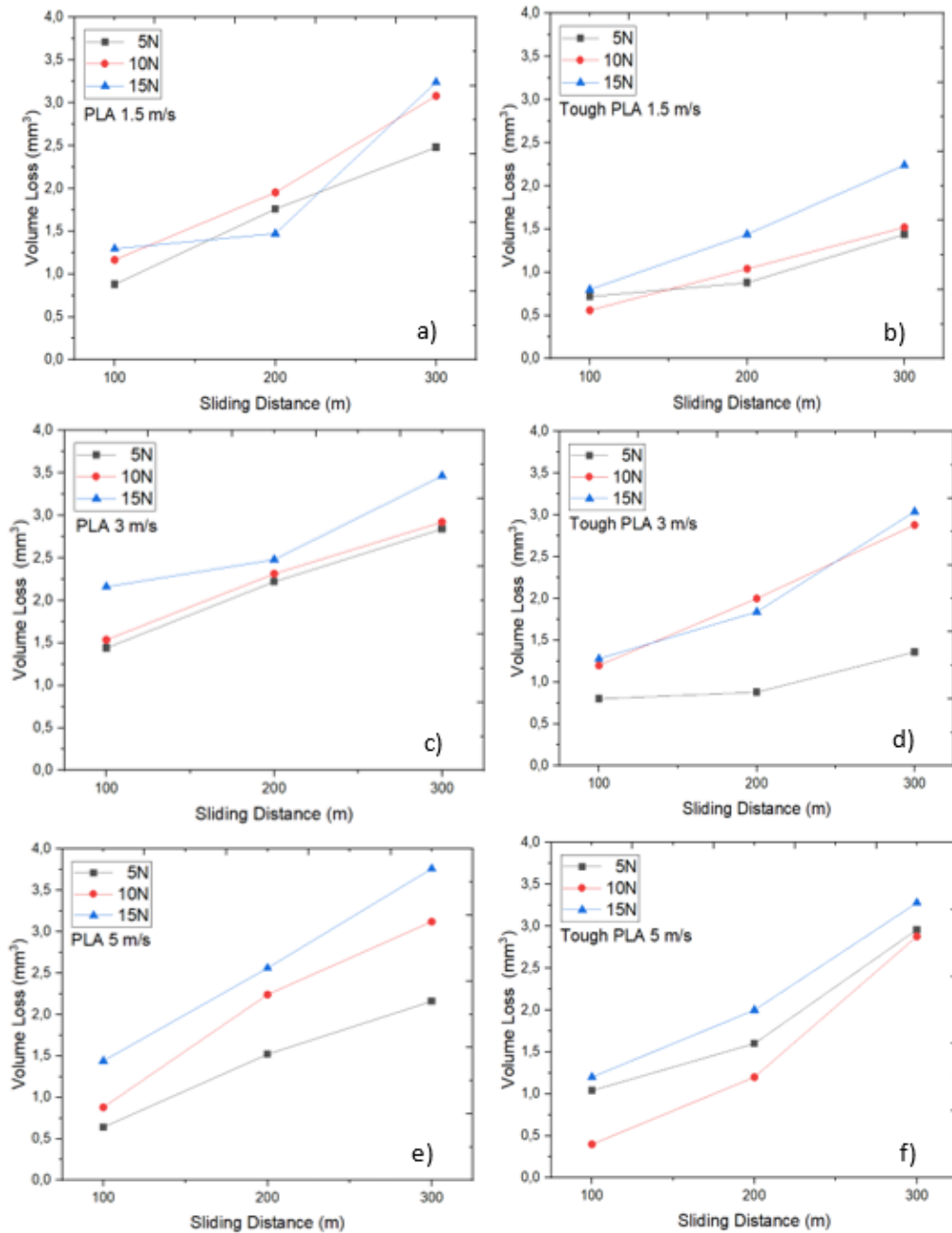


Figure 4. Volume loss of: a) PLA-1.5 m/s, b) Tough PLA-1.5 m/s, c) PLA-3 m/s, d) Tough PLA-3 m/s, e) PLA-5 m/s, f) Tough PLA-5 m/s by distance and load

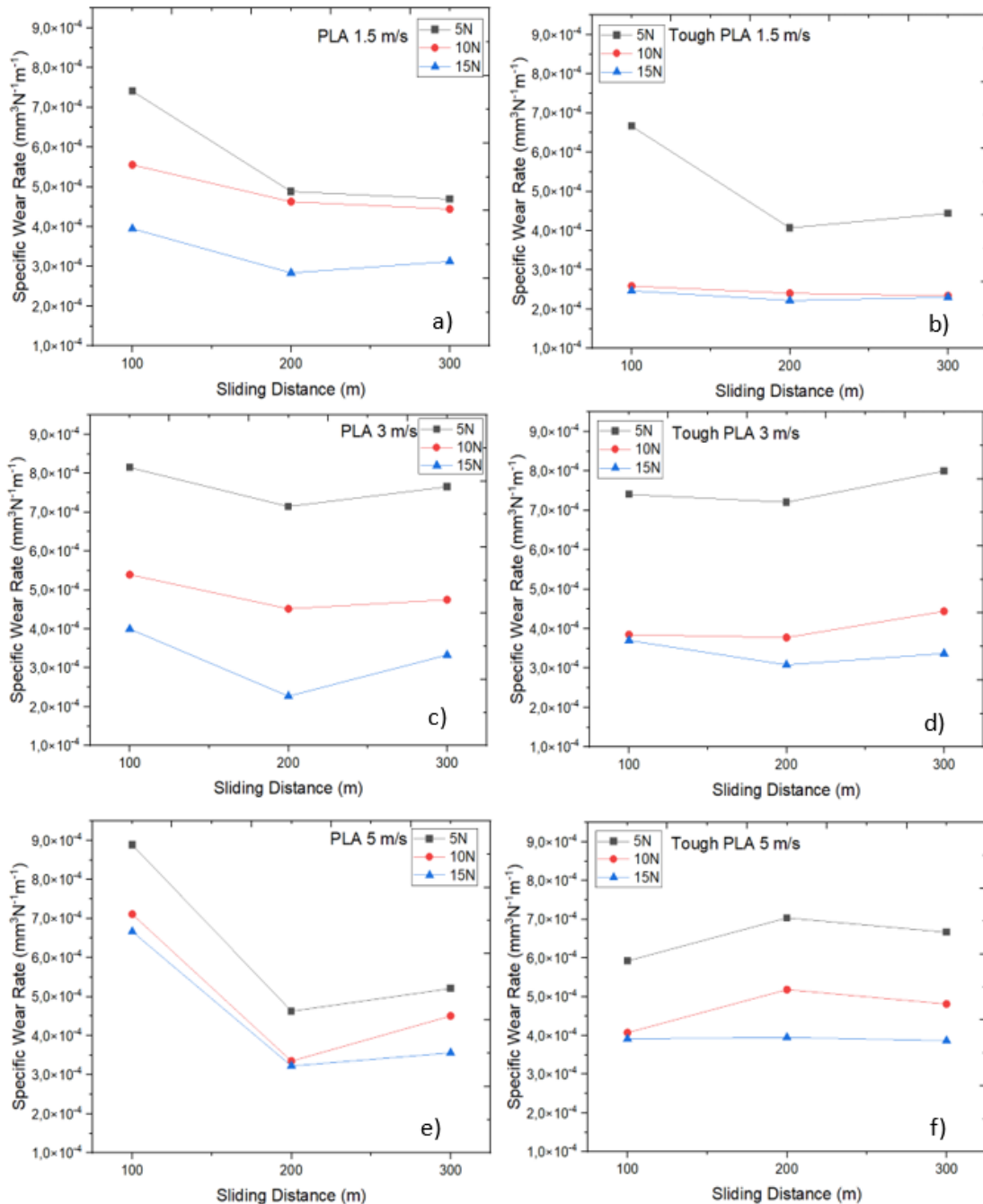


Figure 5. SWR of: a) PLA-1.5 m/s b) Tough PLA-1.5 m/s, c) PLA-3 m/s d) Tough PLA-3 m/s e) PLA-5 m/s f) Tough PLA-5 m/s by distance and load

Conversely, altering the applied normal load leads to a higher SWR value. As previously mentioned, raising the normal load magnifies the kinetic energy engaged in the friction process, which in turn causes the material layers from the polymeric sample to be transferred to the abrasive paper. This phenomenon contributes to a higher rate of wear, as indicated by the elevated SWR value. This transfer contributes to an escalation in the wear rate. Moreover, the generated heat softens the wear surface, resulting in increased sliding resistance and consequently raising the SWR value. The SWR was also assessed for various sliding distances, as depicted in Figure 5. The results suggest that increasing the sliding distances resulted in a decrease in the SWR for PLA and Tough PLA materials. This reduction in wear rate can be attributed to two contributing factors. The decrease in wear rate can be attributed to two factors. Firstly, the surfaces become smoother as the sliding distance increases, resulting in reduced sliding resistance. Secondly, the transferred layers that form during the initial stages of the friction process act as an additional body, effectively functioning as lubricating agent between the surfaces [28, 33]. These combined factors contribute to the decline in the wear rate observed.

CoF is a widely used property for studying the tribological characteristics of engineering materials. Figure 6 presents the CoF values obtained from wear tests conducted on PLA and Tough PLA specimens. The average CoF values range between 0.35 and 0.45. The results indicate a decreasing trend in the average CoF values as the test loads increase. This trend can be attributed to the change in wear mechanisms during testing. Under higher test loads, significant plastic deformation occurs in the initial stages of the wear test. The contact condition in the surface deformation region changes from SiC (abrasive paper)-polymer with partial adhesion to polymer-polymer contact as the sliding period proceeds. Localization of deformation and unevenly distributed partial voids can result in fluctuations in CoF values [2]. The investigation demonstrated that when the normal load is increased, there is a corresponding rise in the CoF due to the generation of heat during the friction process. The generated heat can cause the sample to undergo softening, leading to an increase in the contact region between the surfaces. Chang et al. [34] reported an elevated CoF with rising contact temperature, particularly under high loads. The examination of the experimental data revealed a notable effect of the printing factors on the durability, hardness, and surface characteristics of the components. As a result, these factors directly affect the tribological features displayed by the components. The findings of this research facilitate the selection of appropriate 3D printing settings based on the desired tribological properties, such as CoF and SWR, for the respective parts.

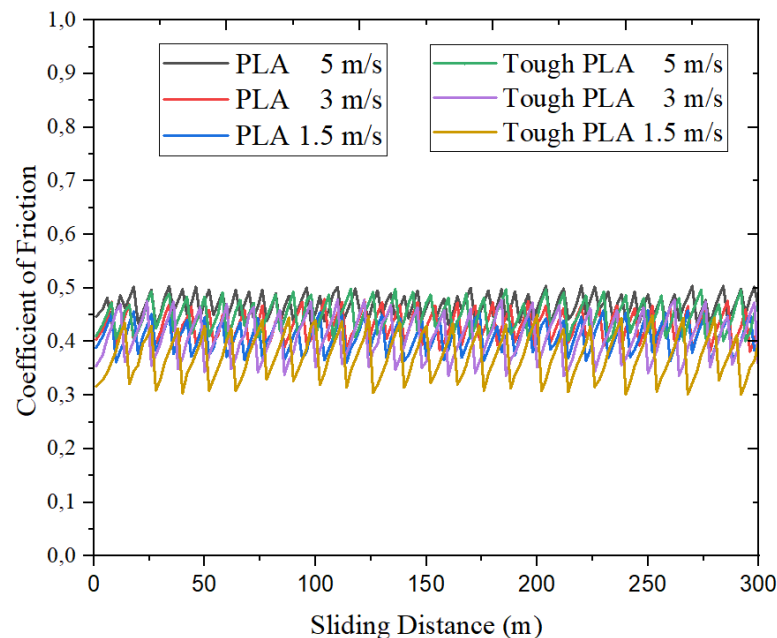


Figure 6. CoF of PLA and Tough PLA by distance

Distinct disparities in the sliding wear characteristics are evident when comparing PLA and Tough PLA materials. Various aspects pertaining to the properties and workability of PLA could be enhanced. These drawbacks encompass inadequate impact strength (low absorbed energy), limited elongation at break (low ductility), low heat deflection temperature (below 60 °C), and challenges in machining (lengthy cycle times and crystallization in processes like injection molding). Employing high-temperature molds becomes necessary to address these concerns [35]. Consequently, PLA exhibits lower wear resistance [36]. The findings from the wear tests further corroborate this observation.

The analysis of the experimental results revealed a notable influence on the wear behavior, extensively discussed within the study. The decline in the CoF can be based on to the sleekness of the specimen surfaces and their interaction with the counter component, specifically noticeable in friction scenarios involving long-distances [37]. Dass et al. [38] proposed that when polymeric samples are subjected to prolonged rubbing against steel discs, the resulting frictional heat can induce localized melting of the polymeric materials. According to their findings, it was observed that the steel disc functions as an intermediate element between the friction surfaces, while a slim polymeric film plays a role in reducing the CoF. A similar phenomenon can be observed in this study, where the SiC paper (abrasive paper),

PLA, and Tough PLA serve as a thin film layer on the sample surface, resulting in a decrease in the CoF.

The volume loss and wear mechanisms map plays an important act in identifying the prevailing mechanisms during wear conditions, enabling the prediction of their impact on the overall wear process. This map is widely utilized for assessing wear mechanisms and their consequences. The increase in sliding distances causes fatigue and micro-fracture mechanisms in wear. In the case of reduced sliding distances, micro-cutting mechanisms occur. The same applies to wear loads. Furthermore, it can be observed that the volume loss decreases at low loads and sliding distances, while it increases at high loads and sliding distances (Figure 7). This information aids in determining suitable wear conditions to enhance wear resistance.

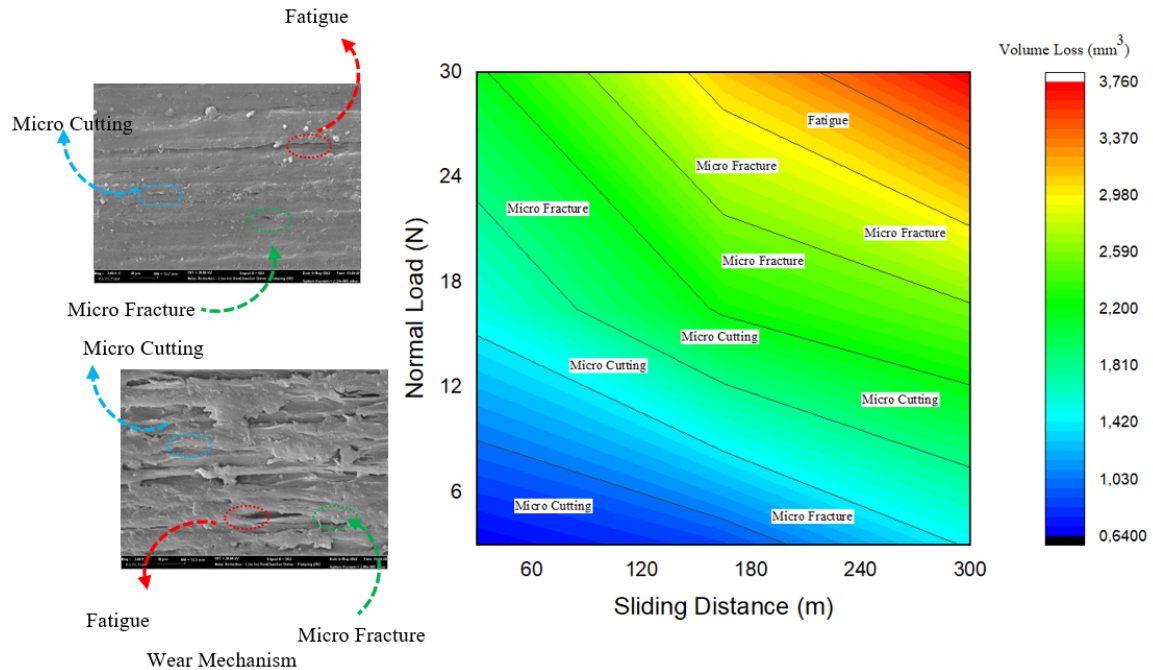


Figure 7. Wear mechanisms map of Tough PLA through volume loss

3.3. Surface roughness analysis

Figure 8 gives the surface roughness results. The data reveals that among the PLA samples, the one with the lowest wear resistance displayed the highest roughness value of $0.981 \mu\text{m}$. On the other hand, the Tough PLA sample, characterized by the highest wear resistance, displayed the lowest roughness value of $0.412 \mu\text{m}$. Particularly, the study observed a significant increase in surface roughness values, particularly under high applied forces. Selecting a 100% infill rate was found to be effective in significantly reducing the measured surface roughness values due to the minimized void volume [2].

Surface roughness has a significant impact on tribological characteristics, affecting them in the following ways: As the surface roughness increases, it reduces the contact area during sliding, leading to elevated pressure and consequently a higher CoF. Conversely, when surface roughness decreases, the sliding contact area expands, leading to a lower CoF. This effect becomes particularly evident in samples with lower loads [29].

When the surface of the test piece exhibits higher roughness, the contact area is diminished, leading to accelerated wear of the superficial layers and, consequently, an increased wear rate. Conversely, an expanded sliding region contributes to a reduced wear rate. This phenomenon has been appropriately described in the tribological investigations conducted on the samples, which included observations of the surface structure under a 15 N load.

The sliding surface of the test piece exhibits a crust texture characterized by peaks and valleys between its layers. These peaks and valleys represent surface roughness, contributing to an overall rough surface. The peaks and valleys of the surface deform during the sliding process, resulting in the building of a different worn surface.

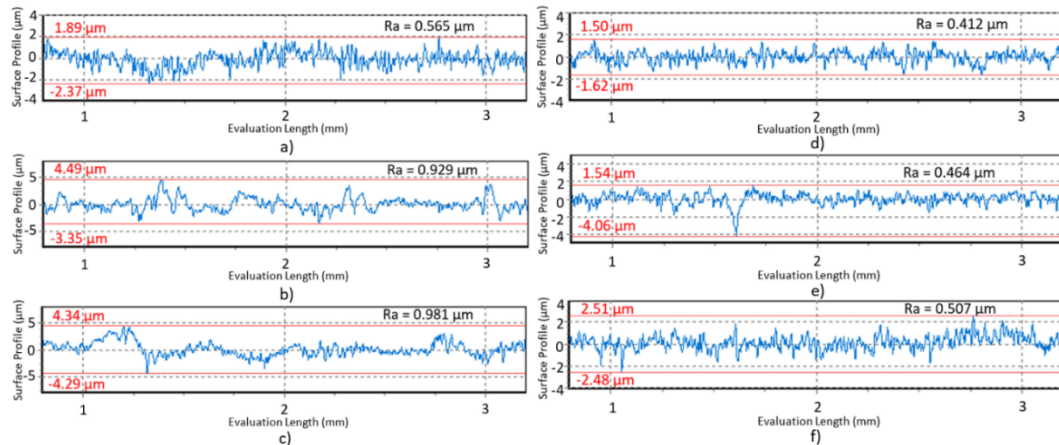


Figure 8. Surface roughness results of: a) PLA-1.5 m/s, b) PLA-3 m/s, c) PLA-5 m/s, d) Tough PLA-1.5 m/s, e) Tough PLA-3 m/s, f) Tough PLA-5 m/s

3.4. Worn surface characterization

The presence of various wear mechanisms, including wear grooves, micro-cutting, micro-fracture, as well as fatigue and plastic deformation, is illustrated in Figure 9 through the SEM analysis of the worn surfaces. These mechanisms are observed in both PLA and Tough PLA samples, with their occurrence dependent on the sliding distance and wear load parameters. Notably, triangular voids are noticeable between the layers throughout the entire thickness of the samples. These voids are likely a result of filament deposition angles between adjacent rasters. SEM image analysis indicated that Tough PLA materials generally exhibit larger voids compared to standard PLA materials (Figure 9). Localized grooves, cavities, and severe abrasion marks were also observed. The development of larger voids in Tough PLA can be caused by a greater amount of plastic deformation as compared with standard PLA, resulting in layer separations. Furthermore, it was observed that the cavities expanded in size as the printing speeds were increased. In the case of Tough PLA samples, gaps between the layers (parallel to the layering direction) were visible. However, it was observed that these gaps closed during production and contact, with plastic deformation increasing under the applied wear load. This study concluded that samples produced with Tough PLA demonstrated improved wear resistance compared to those produced with standard PLA. The higher nozzle temperature also played a role in the superior wear performance of Tough PLA. The varying heating and cooling rates can explain this phenomenon, as PLA was printed at an extrusion temperature of 215 °C while at 225 °C in Tough PLA [14, 39]. Considering the low viscosity of Tough PLA, the increase in extruding temperature resulted in better fluidity and reduced void volume.

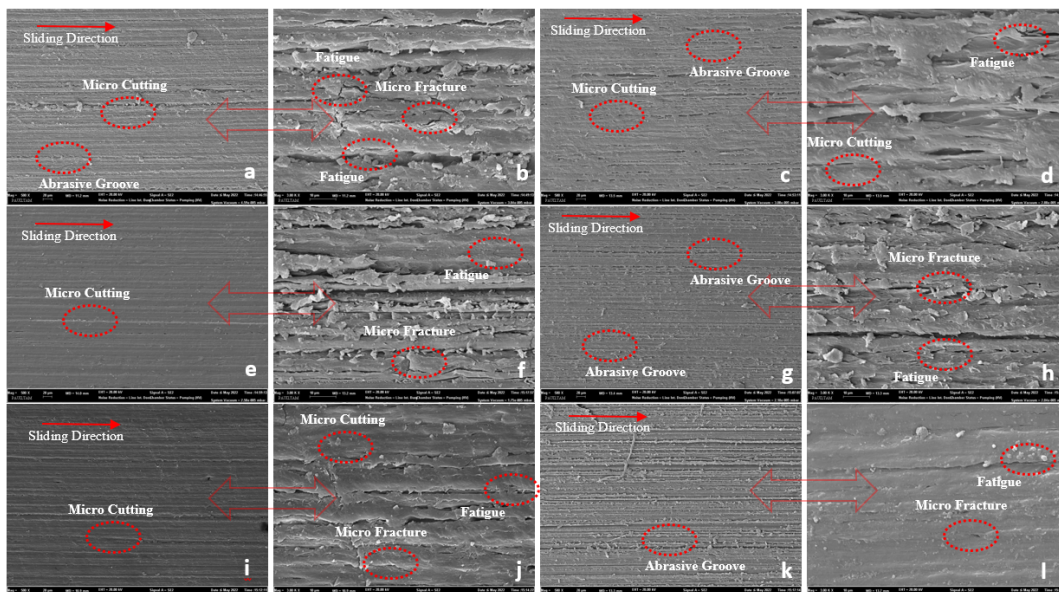


Figure 9. Wear mechanisms of the worn surfaces: (a, b) PLA-1.5 m/s, (c, d) PLA-3 m/s, (e, f) PLA-5 m/s, (g, h) Tough PLA-1.5 m/s, (i, j) Tough PLA-3 m/s, (k, l) Tough PLA-5 m/s (Magnifications are 500x in a, c, e, g, i, k and 3000x in b, d, f, h, j, l)

EDS analysis was performed on the surfaces to gain a particular comment on the effects of wear conditions on wear processes and behavior. The EDS results showed that the presence of abrasive particles in both PLA and Tough PLA samples was not caused by abrasive paper but rather to the formation of polymer-polymer contact areas during the wear test (see Figure 10). SEM-EDS analyses indicated that the wear performance of these samples can be enhanced by optimizing the printing parameters and minimizing internal defects. Parameters such as raster direction, print speed, and nozzle temperature significantly influence the wear resistance of 3D-printed parts. Properly optimizing the process parameters makes it exists to improve the strength and dimensional accuracy of the components by decreasing the gaps formed by the deposited layers [14].

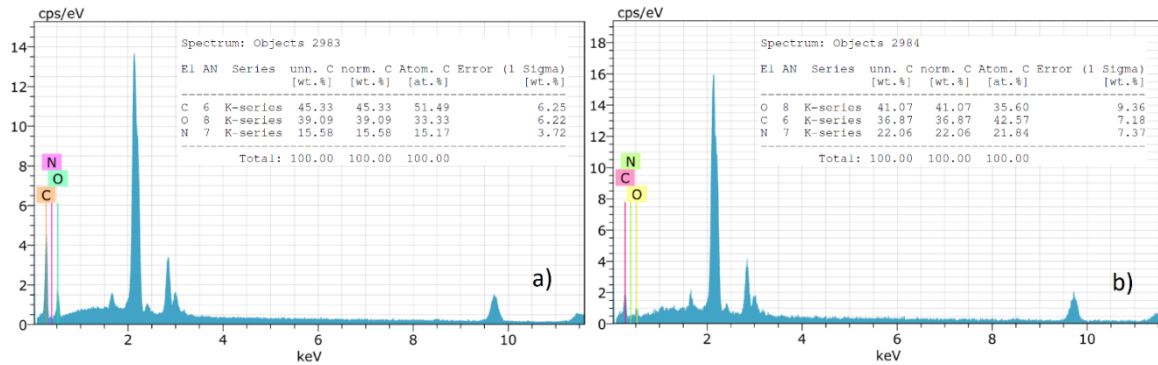


Figure 10. EDS analyses of the worn surfaces: a) PLA-5 m/s, b) Tough PLA-5 m/s

4. Conclusion

The FDM (Fused Deposition Modeling) technique is employed as an efficient and practical means to produce PLA and Tough PLA samples. This method enables the optimization of wear properties within tight tolerances. In this research, the wear characteristics of PLA and Tough PLA materials were thoroughly examined on samples fabricated through 3D printing utilizing the FDM approach. Notably, this study unveils novel insights into the wear mechanisms exhibited by these materials. As a conclusion, the main novel findings are presented following:

- Among the samples produced with 100% infill rate, the PLA sample has a Shore D hardness of 83.6, while the Tough PLA sample has a hardness of 79.3 Shore D.
- Samples produced with Tough PLA showed better wear resistance than those produced with standard PLA.
- The highest volume loss of 3.75 mm³ was observed in the PLA-5 m/s sample under a 15 N load, whereas the lowest volume loss of 0.55 mm³ was observed in the Tough PLA-1.5 m/s sample under a 5 N load. The results support the toughness effect of Tough PLA, with strong interfacial adhesion and a large sliding-deformation tendency with more homogeneously dispersed phases than the PLA matrix.
- Average CoF values tend to decrease with increasing wear load. With the increase of the normal load, the CoF also exhibited an increase.
- In the case of both PLA and Tough PLA samples, increasing the sliding distances reduced the SWR value. However, an increase in the normal load contributes to a higher SWR.
- Based on the detailed surface roughness measurements, it was found that the PLA-5 m/s sample exhibited the highest result of 0.981 μm, while the Tough PLA-1.5 m/s sample displayed the lowest result of 0.412 μm. 100% infill rate led to significantly decreased observed surface roughness values. The surface roughness values increased particularly under high applied forces.
- Analysis of SEM images revealed that, in nearly all samples, Tough PLA materials exhibited larger gaps compared to standard PLA materials.
- The increase in sliding distances causes fatigue and micro-fracture mechanisms in wear. In the case

of reduced sliding distances, micro-cutting mechanisms occur. The same applies to wear loads. Furthermore, it was observed that the volume loss decreases with lower loads and sliding distances, while it increases with higher loads and sliding distances.

Acknowledgment

The author extends their appreciation to Dr. Ismail Ovali for his valuable contributions in providing technical editing and assistance during the writing of this study.

Conflict of Interest Statement

The author declares that there is no conflict of interest.

References

- [1] B. Özlü, O. Pıskı and H. Demir, "Investigation of models produced by rapid prototyping technology solid ground method the dimensional deviations and surface roughness," *Erzincan University Journal of Science and Technology*, vol. 13, no.1, pp. 296-305, March 2020. doi:10.18185/erzifbed.559785
- [2] B. Ergene and Ç. Bolat, "An experimental study on the role of manufacturing parameters on the dry sliding wear performance of additively manufactured PETG," *International Polymer Processing*, vol. 37, no. 3, pp 255-270, April 2022. doi:10.1515/ipp-2022-0015
- [3] E. Zurnacı and H. K. Özdemir, "Investigation of the compressive strength, energy absorption properties and deformation modes of the reinforced core cell produced by the FDM method," *Gazi Journal of Engineering Sciences*, vol. 9, no. 1, pp. 1-11, April 2023. doi:10.30855/gmbd.0705047
- [4] M. Mehrpouya, A. Dehghanghadikolaei, B. Fotovvati, A. Vosooghnia, S. S. Emamian, and A. Gisario, "The potential of additive manufacturing in the smart factory industrial 4.0: A review," *Applied Sciences*, vol. 9, no. 18, p. 3865, September 2019. doi:10.3390/app9183865
- [5] D. Erol, B. Doğan and M. Bozdemir, "The experimental study on examination of the usability of three dimensional printing technologies in tread pattern design of vehicle tires," *Gazi Journal of Engineering Sciences*, vol. 6, no. 1, pp. 62-69, April 2020. doi:10.30855/gmbd.2020.01.06
- [6] D. Rahmatabadi, I. Ghasemi, M. Baniassadi, K. Abrinia, and M. Baghani, "3D printing of PLA-TPU with different component ratios: Fracture toughness, mechanical properties and morphology," *Journal of Materials Research and Technology*, vol. 21, pp. 3970-3981, 2022. doi: 10.1016/j.jmrt.2022.11.024
- [7] J.W. Stansbury and M. J. Idacavage, "3D printing with polymers: Challenges among expanding options and opportunities," *Dental Materials*, vol. 32, no. 1, pp. 54-64, January 2016. doi: 10.1016/j.dental.2015.09.018
- [8] Ü. G. Başçı, and R. Yamanoğlu, "New generation production technology: additive manufacturing via FDM," *International Journal of 3D Printing Technologies and Digital Industry*, vol. 5, no. 2, pp. 339-352, August 2021. doi:10.46519/ij3dptdi.838281
- [9] B. Kaygusuz, and S. Özerinç, "Investigation of mechanical properties of PLA-based structures produced by 3D printer," *Machine Design and Manufacturing Magazine*, vol. 16, no. 1, pp. 1-6, May 2019.
- [10] T. Tabi, I. E. Sajo, F. Szabo, A. S. Luyt, and J. G. Kovacs, "Crystalline structure of annealed polylactic acid and its relation to processing," *Express Polymer Letters*, vol. 4, no.10, pp. 659-668, October 2010. doi:10.3144/expresspolymlett.2010.80
- [11] M. Murariu and P. Dubois, "PLA composites: From production to properties," *Advanced Drug Delivery Reviews*, vol. 107, pp. 17-46, December 2016. doi: 10.1016/j.addr.2016.04.003
- [12] Wu, N. and Zhang, H., "Mechanical properties and phase morphology of super-tough PLA/PBAT/EMA-GMA multicomponent blends," *Materials Letters*, vol. 192, pp. 17-20, April 2017. doi: 10.1016/j.matlet.2017.01.063
- [13] A. Pandzic and D. Hodzic, "Mechanical properties comparison of PLA, tough PLA and PC 3D printed materials with infill structure - Influence of infill pattern on tensile mechanical properties," *The International Conference on Development and Modernization of Manufacturing (RIM), IOP Conf. Series: Materials Science and Engineering, Sarajevo, vol. 1208, pp. 1-13, December 2021. doi:10.1088/1757-899X/1208/1/012019*
- [14] N. Naveed, "Investigating the material properties and microstructural changes of fused filament fabricated PLA and Tough-PLA parts," *Polymers*, vol. 13, no. 9, pp.1487, May 2021. doi:10.3390/polym13091487
- [15] Ultimaker 2022, "Ultimaker tough PLA TDS," *makerbot.com*, Apr. 2022. [Online]. Available: <https://support.makerbot.com/s/article/1667411002379>. [Accessed: Feb. 17, 2023].
- [16] S. S. Karabeyoğlu, O. Ekşi, and K. Feratoğlu "Wear characteristics of PLA-Cu composites manufactured by fused deposition modelling under different temperature conditions," *Journal of Balikesir University Institute of Science and Technology*, vol. 23,

no.1, pp 358-365, January 2021. doi:10.25092/baunfbed.854829

- [17] I. Istif, "Identification of dry sliding wear behaviour of PLA parts manufactured by fused deposition modelling," *Dicle University Journal of Engineering*, vol. 12, no. 2, pp. 275-283, March 2021. doi:10.24012/dumf.855768
- [18] S. Yilmaz, "Comparative investigation of mechanical, tribological and thermo-mechanical properties of commonly used 3D printing materials," *European Journal of Science and Technology*, no. 32, pp. 827-831, 2021. doi:10.31590/ejosat.1040085
- [19] A. Sevil, A. Ondört, S. Ürgün, and S. Fidan, "Powder coating of 3D printed parts surfaces and erosive wear behaviour characterization of coatings," *European Journal of Science and Technology*, vol. 17, pp. 1106-1115, December 2019. doi:10.31590/ejosat.652512
- [20] C. Rajesh, N.K. Venkata, and G. Gowthami, "Evaluation of wear behaviour OFPLA & ABS parts fabricated by operate FDM technique with distinct orientations," *International Journal of Recent Technology and Engineering*, vol. 7, no. 5S3, February 2019.
- [21] M.A. Cuiffo, J. Snyder, A.M. Elliott, N. Romero, S. Kannan and G.P. Halada, "Impact of the fused deposition (FDM) printing process on polylactic acid (PLA) chemistry and Structure," *Applied Sciences*, vol. 7, no. 6, pp. 579, June 2017. doi:10.3390/app7060579
- [22] J.B. Soares, J. Finamor, F.P. Silva, L. Roldo and L.H. Cândido, "Analysis of the influence of polylactic acid (PLA) colour on FDM 3D printing temperature and part finishing," *Rapid Prototyping*, vol. 24, no. 8, pp. 1305-1316(12), January 2018. doi:10.1108/RPJ-09-2017-0177
- [23] P. K. Gurralla, and S. P. Regalla, "Part strength evolution with bonding between filaments in fused deposition modelling," *Virtual and Physical Prototyping*, vol. 9, no. 3, pp. 141-149, May 2014. doi: 10.1080/17452759.2014.913400
- [24] S. Singh, S. Ramakrishna and R. Singh, "Material issues in additive manufacturing: a review," *Journal of Manufacturing Processes*, vol. 25, pp. 185-200, January 2017. doi: 10.1016/j.jmapro.2016.11.006
- [25] K.R. Samit, B. Amritanshu, K.B. Bidyut, P. Debapriya and D. Barnali, 2 - *Tribological analysis-general test standards*, Editor(s): Soney C. George, Jozef T. Haponiuk, Sabu Thomas, Rakesh Reghunath, Sarath P. S., In Elsevier Series on Tribology and Surface Engineering, Tribology of Polymers, Polymer Composites, and Polymer Nanocomposites, Elsevier, 2023, pp. 17-50, doi:10.1016/B978-0-323-90748-4.00001-7.
- [26] D.C. Wijnbergen, M.V.D. Stelt and L.M. Verhamme, "The effect of annealing on deformation and mechanical strength of tough PLA and its application in 3D printed prosthetic sockets," *Rapid Prototyping Journal*, vol. 27 no. 11, pp. 81-89. August 2021. doi:10.1108/RPJ-04-2021-0090
- [27] T. Letcher and M. Waytashek, "Material property testing of 3D-printed specimen in PLA on an entry-level 3D printer," in *ASME 2014, International Mechanical Engineering Congress and Exposition; American Society of Mechanical Engineers: Montreal, vol. 2, December 2014*. doi:10.1115/IMECE2014-39379
- [28] A. Fouly, A.K. Assaifan, I.A. Alnaser, O.A. Hussein and H.S. Abdo, "Evaluating the mechanical and tribological properties of 3D printed polylactic-acid (PLA) green-composite for artificial implant: Hip joint case study," *Polymers*, vol. 14, no. 23, December 2022. doi:10.3390/polym14235299
- [29] M. H. Muammel and Z. László, "Comprehending the role of process parameters and filament color on the structure and tribological performance of 3D printed PLA," *Journal of Materials Research and Technology*, vol. 15, pp. 647-660, November-December 2021. doi: 10.1016/j.jmrt.2021.08.061
- [30] N. Wu and H. Zhang, "Mechanical properties and phase morphology of super-tough PLA/PBAT/EMA-GMA multicomponent blends," *Materials Letters*, vol. 192, pp. 17-20, April 2017. doi: 10.1016/j.matlet.2017.01.063
- [31] S. Perepelkina, P. Kovalenko, R. Pechenko and K. Makhmudova, "Investigation of friction coefficient of various polymers used in rapid prototyping technologies with different settings of 3D printing," *Tribology in Industry*, vol. 39, no. 4, pp. 519-526, December 2017. doi:10.24874/ti.2017.39.04.11
- [32] H. Karakoç, İ. Ovalı, S. Dünder and R. Çitak, "Wear and mechanical properties of Al6061/SiC/B4C hybrid composites produced with powder metallurgy," *Journal of Materials Research and Technology*, vol. 8, no. 6, pp. 5348-5361, November-December 2019. doi:10.1016/j.jmrt.2019.09.002
- [33] N.W. Khun, H. Zhang, L.H. Lim, C.Y. Yue, X. Hu and J. Yang, "Tribological properties of short carbon fibers reinforced epoxy composites," *Friction*, vol. 2, no. 3, pp. 226-239, September 2014. doi:10.1007/s40544-014-0043-5
- [34] L. Chang, Z. Zhang, H. Zhang and K. Friedrich, "Effect of nanoparticles on the tribological behaviour of short carbon fibre reinforced poly (etherimide) composites," *Tribology International*, vol. 38, no. 11-12, pp. 966-973, November 2005-December 2006. doi: 10.1016/j.triboint.2005.07.026
- [35] K. Hashima, S. Nishitsuji and T. Inoue, "Structure-properties of super-tough PLA alloy with excellent heat resistance," *Polymer*, vol. 51, no. 17, pp. 3934-3939, August 2010. doi: 10.1016/j.polymer.2010.06.045.
- [36] R. Muntean, S. Ambruş, N.-A. Sirbu and I. D. Uşu, "Tribological properties of different 3D printed PLA filaments," *In Nano Hybrids and Composites*, vol. 36, pp. 103-111, June 2022. doi: 10.4028/p-8k2v92

[37] S.Z. Hervan. A. Altinkaynak and Z. Parlar, "Hardness, friction and wear characteristics of 3D-printed PLA polymer," *Proceedings of the Institution of Mechanical Engineers, Part J: Journal of Engineering Tribology*, Vol.235, no. 8, pp. 1590-1598, October 2020. doi:10.1177/1350650120966407

[38] K. Dass, S.R. Chauhan and B. Gaur, "Study on the effects of nano-aluminum-oxide particulates on mechanical and tribological characteristics of chopped carbon fiber reinforced epoxy composites," *Proceedings of the Institution of Mechanical Engineers, Part L: Journal of Materials: Design and Applications*, vol. 231, no. 4, pp.403-422, 2017. doi:10.1177/1464420715598798

[39] A.K. Sood, R.K. Ohdar and S.S. Mahapatra, "Parametric appraisal of mechanical property of fused deposition modelling processed parts," *Materials & Design*, vol. 31, no. 1, pp. 287-295, January 2010. doi: 10.1016/j.matdes.2009.06.016

This is an open access article under the CC-BY license

